Check for updates

RESEARCH ARTICLE

Analytical assessment and overview of copper-coated secondary elements in linear induction motors as a rare-earth free motor option for transportation systems

[version 1; peer review: awaiting peer review]

Areg Khangeldyan[1], Hayk Akarmazyan[2], Vrezh Hayrapetyan[3], Vardan Hovhannisyan[1], Gagik Soghomonyan[2], Karen Melikyan[2]

[1]Chair of Electrical Machines and Apparatus, National Polytechnic University of Armenia, Yerevan, Yerevan, 0009, Armenia
[2]National Polytechnic University of Armenia, Yerevan, Yerevan, 0009, Armenia
[3]Scientific Research Institute of Energy CJSC, Yerevan, Yerevan, 0025, Armenia

v1 **First published:** 20 Oct 2026, **6**:439
https://doi.org/10.12688/openreseurope.25110.1
Latest published: 20 Oct 2026, **6**:439
https://doi.org/10.12688/openreseurope.25110.1

Abstract

Background

In the context of the global transition to renewable energy sources, the development of technologies that remain sustainable throughout their entire life cycle and do not depend on critical materials has become particularly significant. In this regard, linear induction motors (LIM) are considered an alternative to permanent-magnet drives, which require rare-earth elements. Copper-coated solid secondary elements may improve LIM electromagnetic performance while maintaining a rare-earth-free design.

Methods

This study analyzes the feasibility of using copper-coated solid secondary elements to enhance LIM electromagnetic performance. A review of existing research on copper coating deposition, its properties and application to solid secondary elements is provided, with attention to cold gas dynamic spray deposition of copper onto iron. LIM parameters for a high-speed transportation system were calculated analytically using a corrected Γ-shaped equivalent circuit and the complex magnetic resistance approach. The characteristics of the conventional design were compared with those of versions employing copper-coated solid secondary elements. The copper-layer thickness varied from 0 to 0.002 m.

Open Peer Review

Approval Status *AWAITING PEER REVIEW*

Any reports and responses or comments on the article can be found at the end of the article.

Results

The analysis demonstrates that the use of copper-coated solid secondary elements is a promising approach to improving the performance of LIMs without relying on rare-earth materials. Compared with the uncoated secondary element, thrust force decreased at a copper thickness of 0.0001 m and then increased with coating thickness. Favorable changes in operating slip, vehicle velocity, power factor and efficiency were also observed with increasing copper-layer thickness.

Conclusions

Copper-coated solid secondary elements show potential for improving the electromagnetic characteristics of LIMs without significant structural modifications. Further studies are needed to optimize the copper-layer thickness, evaluate thermal, mechanical and edge effects, and validate the results through experimental testing and FEM analysis. The proposed approach may support the development of reliable and environmentally sustainable rare-earth-free drive systems for transportation and industrial applications.

Plain Language summary

As countries move toward renewable energy, there is a growing need for technologies that are efficient, environmentally sustainable and less dependent on materials that may be difficult to obtain. Linear induction motors (LIM) are one possible alternative to permanent-magnet motors because they do not require rare-earth materials. However, improving their performance remains an important challenge.

In this study, we investigated whether adding a thin copper coating to the solid secondary element of a LIM could improve its performance. We reviewed previous research on copper coatings, including methods for applying copper to iron, and then analyzed a LIM designed for a high-speed transportation system. Different copper-layer thicknesses, from 0 to 0.002 m, were considered and compared with a conventional uncoated design.

The results showed that the copper coating can affect several important characteristics of the LIM. The thrust force initially decreased at a copper thickness of 0.0001 m and then increased as the coating became thicker. Increasing the copper-layer thickness also resulted in favorable changes in operating slip, vehicle velocity, power factor and efficiency.

These findings suggest that copper-coated solid secondary elements could improve the electromagnetic characteristics of LIMs without significant structural modifications. Further research is needed to optimize the copper-layer thickness and evaluate thermal, mechanical

and edge effects. Future studies will also include experimental testing and FEM analysis to validate the results. This approach may support the development of reliable and environmentally sustainable rare-earth-free electric drive systems for transportation and industrial applications.

Keywords
Cold spray deposition, linear induction motor, solid secondary element, electromagnetic parameters, transportation systems, rare-earth-free motors, copper coating.



This article is included in the Horizon Europe gateway.

Corresponding author: Areg Khangeldyan (aregkhangeldyan@polytechnic.am)

Author roles: Khangeldyan A: Conceptualization, Investigation, Methodology, Resources, Validation, Visualization, Writing – Original Draft Preparation; **Akarmazyan H**: Conceptualization, Supervision, Writing – Review & Editing; **Hayrapetyan V**: Writing – Original Draft Preparation; **Hovhannisyan V**: Writing – Original Draft Preparation; **Soghomonyan G**: Writing – Original Draft Preparation; **Melikyan K**: Investigation, Writing – Original Draft Preparation

Competing interests: No competing interests were disclosed.

Grant information: This project has received funding from the European Union's Horizon Europe research and innovation programme under grant agreement No. [101159235] (project name: Strengthening Research in Armenia for Energy Transition toward Climate Solutions [STREACS]). The funders had no role in the study design, data collection and analysis, decision to publish, or preparation of the manuscript.
The funders had no role in study design, data collection and analysis, decision to publish, or preparation of the manuscript.

Copyright: © 2026 Khangeldyan A *et al*. This is an open access article distributed under the terms of the Creative Commons Attribution License, which permits unrestricted use, distribution, and reproduction in any medium, provided the original work is properly cited.

How to cite this article: Khangeldyan A, Akarmazyan H, Hayrapetyan V *et al.* **Analytical assessment and overview of copper-coated secondary elements in linear induction motors as a rare-earth free motor option for transportation systems [version 1; peer review: awaiting peer review]** Open Research Europe 2026, **6**:439 https://doi.org/10.12688/openreseurope.25110.1

First published: 20 Oct 2026, **6**:439 https://doi.org/10.12688/openreseurope.25110.1

1. Introduction

Owing to continuous technological progress and the rapid expansion of electrification, the application scope of LIMs has increased significantly in recent years. These machines are increasingly deployed in industrial automation, transportation systems, renewable energy infrastructure, and other demanding applications where high reliability and operational stability are required.[1–3] Consequently, LIMs are often exposed to harsh operating environments involving elevated mechanical and thermal stress, leading to intensified loading conditions and stricter performance requirements. This trend has created a growing need to improve the mechanical durability of the secondary element while simultaneously enhancing its electrical and magnetic characteristics.

Traditionally, high-performance electric machines have relied on permanent magnet technologies that depend on critical raw materials (CRMs), particularly rare-earth elements such as neodymium and dysprosium. While these materials enable high efficiency and torque density, their extraction and processing are associated with significant environmental impacts, including water contamination, hazardous waste generation, and high energy consumption. In addition, global supply chains for rare-earth elements remain geographically concentrated, creating economic and geopolitical vulnerabilities.[4] As a result, increasing attention is being directed toward the development of rare-earth-free electric machine technologies capable of achieving comparable performance while reducing dependence on CRMs.

Within this context, induction motors represent a promising alternative due to their robustness, scalability, and relatively simple construction. However, achieving higher efficiency and improved electromagnetic performance requires optimization of the rotor and secondary element properties. These characteristics are strongly linked to the properties of the materials used and to the surface quality of the secondary element. Therefore, more stringent requirements are imposed on the base materials, their parameters, and their functional performance. To meet modern operational and sustainability requirements, the surface of the secondary element must therefore exhibit optimized mechanical, electrical, and magnetic properties while also supporting lifecycle sustainability and resource efficiency objectives.

Recent studies indicate that copper-coated iron structures can provide an effective balance between magnetic permeability and electrical conductivity, enabling reduced eddy current losses, improved thermal stability, and enhanced thrust characteristics..[5] Currently, various copper-deposition techniques are known,[6] including electroplating and cold spray deposition, which allow the production of high-quality coatings. To improve the electromagnetic parameters of electric machines, copper-coated secondary elements with different coating thicknesses are employed. These coatings form an additional conductive path in the LIM equivalent circuit and enable achieving specific electrical resistivity and magnetic permeability within the desired range.[7] These parameters directly influence the starting and operational characteristics of LIMs. Such motors can be used in transportation systems to improve their performance, particularly in high-speed rail transportation systems.

Previous research has demonstrated the potential benefits of copper-coated iron secondary elements for enhancing the electromagnetic performance of linear induction motors. However, the relationship between copper coating thickness and LIM performance has not been comprehensively quantified. In particular, the influence of coating thickness on key operating parameters, including efficiency, power factor, and overall machine performance, remains insufficiently understood. This study therefore aims to investigate the potential of copper-coated solid secondary elements for improving the electromagnetic and mechanical performance of LIMs, while also evaluating their applicability as a rare-earth-free alternative to conventional high-performance motor technologies. Particular attention is given to the effect of copper coating thickness on performance enhancement from the perspective of sustainable and resource-efficient electric machine design.

2. Literature review

In modern urban and intercity rail transport systems, numerous applications of linear electric drives have been developed and implemented. Among them, particular attention is given to LIMs and linear synchronous motors (LSMs) with permanent magnets.[8,9] Depending on operational requirements and application conditions, both motor types are successfully employed in railway systems of varying purposes, structures, and speed ranges, including both low-speed and high-speed transport.[8–10] Resent research in that field is focused on improving their design and operating parameters for transportation[8,9] as well as for broader industrial applications.[11]

In the context of maglev transportation systems, both LIM and LSM drives present distinct advantages and limitations.[8–10] Although LSM-based propulsion systems require a more expensive guideway infrastructure, they remain one of the preferred practical solutions for high-speed operation (exceeding 200 km/h).[8–10] In contrast, LIM systems face increasing challenges at high speeds due to the weight and complexity of onboard power conditioning equipment, as well as difficulties in transferring high electrical power efficiently.[8,9] However, at lower speeds ($\leq$100 km/h), LIM drives have

demonstrated reliable and cost-effective all-weather performance in both maglev and conventional steel-wheel railway systems. For intermediate speeds around 200 km/h, the selection between LIM and LSM technologies depends largely on lifecycle cost considerations.[8,9] LIM technology benefits from its similarity to conventional rotary motor systems widely used in railways, enabling easier integration and leveraging existing engineering experience. Additionally, LIM systems feature relatively simple guideway constructions, resulting in lower infrastructure costs, reduced maintenance requirements, and high operational flexibility. Although LIM systems generally exhibit lower efficiency and power factor compared to LSM systems, recent research is focused on reducing this gap.[8,9]

One of the specifications of LSMs is permanent magnet LSM (PM-LSM). Permanent magnets have been widely applied in LSMs, particularly in industrial automation and transportation systems. Their use in urban maglev propulsion is also expanding.[8,9] Advances in rare-earth magnetic materials, especially neodymium-iron-boron (Nd-Fe-B) and samarium-cobalt (Sm-Co), have enabled high-performance motor designs due to their high magnetic energy density, strong remanent magnetization, and high coercivity. Transportation systems based on PM-LSMs are characterized by high efficiency and high thrust force, making them suitable for high-speed applications.[8,9] Their control systems are analogous to those used in conventional rotary synchronous motors, allowing the reuse of established servo control technologies.[9] Structurally, PM-LSMs resemble linear pulse motors and may be considered a specialized form within this class. However, such systems are typically designed for specific applications rather than standardized deployment. Nowadays, certain successes are known in the implementation of PM-LSMs in high-speed transport systems and studies of improving their construction.[8–10] However, compared with LIMs complex construction of transportation systems with PM-LSMs remains one of the important engineering challenges.[9,10] Robust support and fixation structures are necessary to withstand strong magnetic forces. Furthermore, environmental factors such as temperature variations and corrosion also should be considered. Especially permanent magnets need protective measures from environmental factors, which may reduce magnetic performance.[9] Besides, the requirement for larger permanent magnet components complicates magnet manufacturing, particularly achieving uniform magnetization, and increases mechanical stresses within the system. As a result, the initial investment for PM-LSM-based systems remains relatively high, particularly due to the specialized nature and limited production scale of large rare-earth magnet components.[9] From an environmental and sustainability perspective, the use of PM-LSMs also presents challenges. These include the environmental impact of rare-earth material extraction, processing difficulties, and the limited geographical distribution of key resources, which are concentrated in a small number of countries.[12,13]

An important application of copper coating is in induction motors. Of particular interest are the solid rotors of rotating induction motors and secondary elements of the LIMs (Figure 1). As shown in,[5] in transport LIMs, copper-coated secondary elements are used to enhance the electromagnetic coupling between the primary and secondary circuits, thereby improving electromagnetic parameters.[5] One approach to structural improvement of electrical machines has been proposed in.[14] In,[14] a method for manufacturing stacked magnetic cores for electrical machines is presented, in which, for the reliability of the magnetic core attachment, the assembly of the stack is implemented using uniform metal coating deposition by spraying.[14] Copper coating can be applied to ensure high speeds in rotating induction motors.[15] Copper plating can increase output power and reduce the rotor resistance.[7]

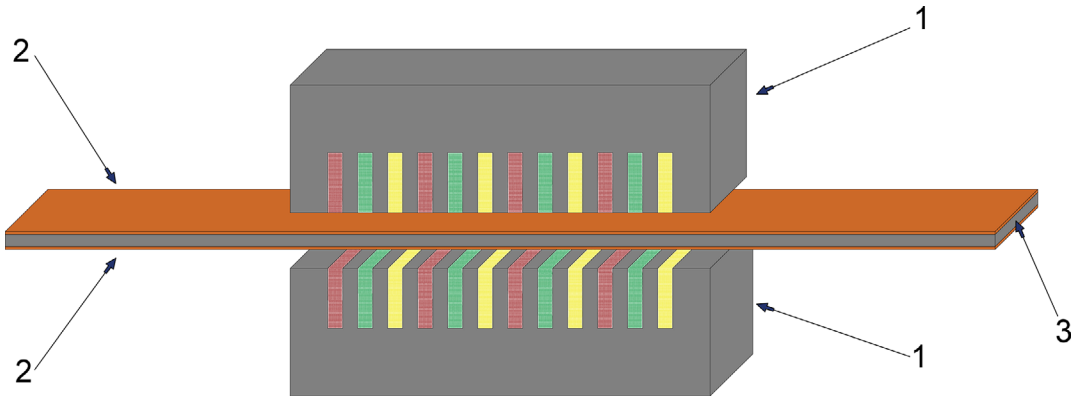

Figure 1. Top view of a double-sided LIM with a copper-plated solid secondary element. 1. Double-sided stator with a three-phase winding. 2. Copper layer. 3. Solid iron secondary element. The double-sided LIM consists of a short stator and a long secondary element. The secondary element is made of solid iron and is copper-plated on both sides. The stator incorporates a three-phase winding that produces the travelling magnetic field. Each phase winding was represented by a single color.

Currently, significant research attention is focused on LIMs with copper-coated secondary elements.[16–19] These studies aim to improve the electromagnetic and mechanical characteristics of motors. Table 1. presents LIM configurations with iron secondary elements of varying thickness (iron thickness - Δ_h) coated with copper layer (copper layer thickness - Δ_{Cu}).

Studies[16–19] focus on improving the thrust force, power factor, and efficiency (η) of LIM. Although the listed LIMs have different nominal powers, thrust forces, and dimensions, the objectives of improving these parameters can be achieved by copper plating the secondary element.[16–19]

Currently, several methods for applying metal coatings to the surface are known, such as cladding, plating, and spraying techniques. These methods are further subdivided depending on the application and properties of the material. In recent years, additive manufacturing-based coating methods have also been actively utilized.[6,20]

It is worthwhile to consider the method of galvanic copper deposition separately. This method represents an electrochemical process of applying a copper coating to a surface.[21] One limitation of this method is the potential for non-uniform thickness distribution of the deposited coating across the surface.[21] More uniformity in the coating can be achieved by using additional anodes and shielding elements, as well as by utilizing the «throwing power» (ability of the electrolyte to produce uniform coatings) of the electrolyte, which depends on the electrolyte's electrical conductivity and polarization characteristics.[21]

Depending on the application, the listed methods are successfully used to obtain coatings for various purposes. In addressing the objective, it is important that the microstructure and properties of both the coating material and the substrate remain as unchanged as possible. In addition, internal stresses and deformations in the product must be avoided and the coating process should be technologically simple, easy to implement and suitable for use under field conditions. A method that best satisfies these requirements is cold gas dynamic spray (CGDS).[22,23] CGDS is a type of gas-dynamic spraying, the essence of which lies in accelerating particles of powdered material in a carrier gas to supersonic speeds using a Laval nozzle or its modifications. The particles, accelerated by the gas flow, impact with the treated surface and adhere to it. Pure ductile metals, as well as mechanical mixtures of metallic, ceramic, or polymer powders, can be used for coating deposition. In the CGDS process, particle velocity is mainly controlled by adjusting the gas pressure, while the gas temperature varies within a limited range and remains significantly below the melting temperature of the particles, preventing melting and excessive heating of the substrate. It is important to note that, compared with other technologies, the CGDS method has several significant advantages:

- The coating application process does not induce significant thermal effects in the substrate. As a result, internal stresses, deformations, and changes in mechanical properties are minimized or eliminated.
- During the coating deposition, the surface is cleaned of technical contaminants, oils, and paints, which facilitates an improved coating process.
- Coatings can be applied to localized areas of the surface.

Coatings can be deposited under both stationary and field conditions, in ambient air at atmospheric pressure, and the process is relatively environmentally friendly.[6,22–25]

Table 1. Variants of LIM with copper-plated secondary element.

Motor type	Specification of secondary element
LIM[16]	Flat steel magnetic core Δ_h = 8 mm with Δ_{Cu} = 2 mm copper layer
LIM[17]	Flat steel magnetic core with Δ_{Cu} = 5 mm and Δ_{Cu} = 10 mm copper layers
LIM[18]	Magnetic core Δ_h = 6 mm made of three 2 mm thick steel plates (St-3), copper-plated with Δ_{Cu} = 3 mm layer
LIM[19]	Flat steel magnetic core Δ_h = 8 mm with Δ_{Cu} = 3 mm copper layer

Note: Table 1. summarizes the variants of LIMs with copper-plated secondary elements reported in the literature. The table presents different secondary element configurations and copper layer thicknesses investigated in previous studies.

From a chemical perspective, CGDS coating technique has significant advantages due to its solid-state nature.[26–28] In contrast to conventional thermal spraying, which relies on high temperatures, cold spray operates below the melting point of the feedstock material,[26,27] preventing oxidation, decomposition, and undesirable phase transformations while preserving chemical purity and much of the original microstructure.[26,29] This is especially important for metals prone to oxidation, such as copper.[30,31] The relatively low processing temperature also limits thermal interaction with the substrate, thereby reducing the likelihood of heat-affected zones, excessive diffusion, residual stress development, and microstructural changes,[28,32] making the technique suitable for temperature-sensitive components and multilayer systems.

From an environmental perspective, cold spray can be considered a relatively cleaner and more sustainable alternative to other coating technologies.[28,32] The process operates without combustion or plasma generation, thereby avoiding significant emissions such as nitrogen oxides (NOx), volatile organic compounds (VOCs), and carbon monoxide (CO), which are typical of thermal spraying and electroplating processes.[28,32] It also reduces material waste through efficient particle delivery, enabling powder recycling and minimizing overspray, while enclosed operation limits worker exposure to hazardous substances and airborne particles, improving occupational safety and reducing environmental and health impacts.[32] However, the process is not inherently low in energy consumption, as it requires high-pressure gases and powerful compressors to accelerate particles to supersonic speeds,[27,32] and in some cases, depending on system, may demand more energy than conventional thermal spray methods. Nevertheless, the absence of combustion and molten materials eliminates fuel-related emissions and reduces the need for extensive post-processing or fume extraction systems.[28,32]

The chemical behavior of copper under cold spray conditions makes it an excellent candidate for applications requiring high electrical and thermal conductivity.[30] Due to the solid-state nature of the process, oxidation is significantly limited compared to thermal spraying, resulting in substantially lower oxygen contents in cold-sprayed copper coatings.[30] During deposition, copper particles undergo severe plastic deformation upon high-velocity impact, forming dense coatings through solid-state metallic bonding without melting, which minimizes oxidation and porosity while enabling high electrical conductivity.[29–31] Copper is also a recyclable and relatively abundant material, and cold spray enables its efficient utilization while minimizing waste.[32] Furthermore, the process eliminates the need for chemical etching, electroplating baths, and hazardous solvents, significantly reducing environmental impact compared to conventional methods that involve heavy metal ions and generate toxic sludge.[28,32]

Taking into account the above considerations, LIMs with copper coated secondary elements can be regarded as a promising solution for railway transportation systems. In addition to offering competitive performance and cost advantages, such systems avoid the use of rare-earth materials, thereby mitigating environmental concerns, supply risks, and resource concentration issues associated with permanent magnet technologies.

Existing studies on copper coatings discuss that such coatings may improve the electromagnetic characteristics of LIMs while also enhancing the functional properties of coating systems, including composite coating applications.[6,23,33,34] In these cases, the copper layer may act as the primary surface exposed to corrosion, wear, and environmental effects, while remaining relatively easy to restore or replace. In LIMs, wear may occur on secondary elements operating under conditions of mechanical interaction and aggressive environmental exposure. When a copper-coated secondary element is used, degradation primarily affects the copper layer, which functions as a replaceable surface. Restoration of the copper coating may be technologically simpler and more cost-effective than manufacturing a new iron secondary element, potentially reducing maintenance costs and improving system durability and maintainability. Furthermore, the mobility and technological flexibility of CGDS systems enable local restoration of conductive surfaces and geometric dimensions, which may be beneficial for transport infrastructure maintenance and for small-sized LIM applications where structural modifications are limited.

3. Materials and methods

Improving the quality, reliability, and electromagnetic performance of LIMs remains an important objective. For coating the secondary element, both the selection of the coating material and precise control of the deposition thickness at the sub-millimeter scale are critical. This is primarily due to the influence of the coating layer on the electrical and magnetic parameters of the LIM. In addition, non-uniform thickness of the deposited layer may lead to significant distortion of the magnetic field, when the motor operates with small air gaps. Considering these factors and literature review results, copper was selected as the coating material for the solid iron secondary element of the LIM. The selection was determined by the combination of high electrical and thermal conductivity, good ductility, favorable adhesion to metallic substrates, and the possibility of depositing relatively thick conductive layers.[21] In addition, the CGDS method was chosen as the

deposition technique due to its limited thermal impact on the substrate, low oxidation level, and suitability for applying conductive coatings with controlled thickness.

To evaluate the impact of applying a copper coating, new additional calculations were performed based on previous research methodology.[35] The secondary element parameters of the LIM were determined analytically using the corrected Γ-shaped replacement equivalent circuit scheme of an induction motor with a solid secondary element.[36] This approach is based on the concept of complex magnetic resistance, which depends on the electrical conductivity of the magnetic circuit, magnetic permeability, frequency, and geometrical parameters.[36] The presence of the copper layer was incorporated into the equivalent circuit, as described in.[35] Specifically, an additional parallel branch was introduced in the secondary circuit to represent the active resistance of the copper coating, while the reactance of the coating was neglected.[35] The calculation procedure follows established methodologies from,[35,37] where[37] addresses LIMs with solid secondary elements, while[35] analyses the composite secondary elements with a copper coating. End effects and mechanical aspects were not considered in the calculations.

The LIM parameters and performance characteristics were calculated analytically according to the following procedure:

- calculating the stator parameters based on the initial conditions,
- determining the active and reactive resistances of the secondary element using the complex magnetic resistance approach,
- determination of the LIM operating parameters and performance characteristics using the equations (1–9) and the procedures described in Annex 1.[38]

The stator parameters were calculated using standard methods based on the Γ shape equivalent circuit schemes of induction motors as described in classical machine theory.[39] Calculations of losses and efficiency were carried out using the principles and equations presented in,[37] while the parameters of the secondary element, thrust force, and critical slip were determined based on the complex magnetic resistance approach described in.[35,36] The thrust force was determined:

$$F_T = F_{Tcr} \times \frac{2(1+q)}{\left(\sigma\sqrt{\frac{s}{s'_{cr}}}+\frac{1}{\sigma}\sqrt{\frac{s'_{cr}}{s}}+2q\right)} \tag{1}$$

where s_{kr} is the critical slip, which can be calculated:

$$s_{cr} = \left(\frac{\sigma r_2}{x_1}h\right)^2 \tag{2}$$

where r_2 is the equivalent active resistance of the secondary element referred to the stator and its values are provided in,[35] F_{Tcr} is the critical thrust force and q, h are coefficients which are related to stator and rotor active and reactive resistance and taken from the theory of complex magnetic resistance. All these parameters were determined using the complex magnetic resistance approach described in.[35,36] The σ is the correction factor, which can be calculated from:

$$\sigma = \sqrt{\left(1+\frac{x_1}{x_\mu}\right)^2+\left(\frac{r_1}{x_\mu}\right)^2} \tag{3}$$

Where r_1 and x_1 active and reactive resistances of the stator winding, and x_μ magnetic reactance of air gap and was calculated using the following equation:

$$x_\mu = 2mf_s\frac{\mu_0 2p\tau l_\delta}{k_\mu k_\delta \delta}\left(\frac{W_1 k_w}{p}\right)^2 \tag{4}$$

where m is the number of stator phases, f_s supply frequency, p number of pole pairs, τ pole pitch, l_δ width of stator, δ air gap, W_1 is the number of turns in the stator winding, k_μ, k_δ and k_w are saturation, air gap and winding coefficients respectively. These parameters and r_1 and x_1 active and reactive resistances, as described earlier are calculated using the classical equivalent circuit scheme of electrical machines.[5,39]

The operating slip was determined by solving the equivalent circuit equations under the condition of nominal stator current, whereas the power factor and the linear velocity of the vehicle were determined using established methods reported in.[7,36,39] The operating slip was determined at the rated stator current from the stator current-slip characteristic. According to the equivalent circuit[36,39] of the induction motor, the stator current can also be expressed as the phasor sum:

$$\dot{I}_1 = \dot{I}_2'' + \dot{I}_\mu \tag{5}$$

Where I_μ is the magnetizing current and I_2' is the secondary current referred to the stator, which was evaluated using approach described in.[39]

The stator current magnitude is represented as a vector sum of its active and reactive components:

$$|\dot{I}_1| = \sqrt{I_{1a}^2 + I_{1x}^2} \tag{6}$$

Where I_{1a} and I_{1x} are the active and reactive components of the stator current, respectively. The power factor is determined as:

$$cos\varphi = \frac{I_{1a}}{|\dot{I}_1|} \tag{7}$$

Linear velocity of the vehicle is defined as:

$$v_{op} = v_s\left(1 - s_{op}\right) \tag{8}$$

Where v_s is the synchronous velocity of the magnetic field and s_{op} is the operating slip of the LIM. Efficiency of the LIM can be calculated:

$$\eta = 1 - \frac{\sum P}{F_{Top} v_{op} + \sum P} \tag{9}$$

Where F_{Top} and v_{op} are the operating thrust force of the LIM and velocity of vehicle. P is the summary of losses of the LIM, which can be evaluated according to approach described in the.[37] P include stator winding and iron core losses, secondary element losses and additional losses which include mechanical and additional magnetic losses.

The described methodology was applied to a practical case study. The calculations were performed for a LIM designed for a railway transportation system. This allows assessing how the copper coating improves electromagnetic coupling and overall motor performance. LIM configuration was selected with a double-sided short stator and a long secondary element (Figure 1). Carbon structural steel (Steel-3) was selected as the material of the solid secondary element, both without coating and with copper coatings of various thicknesses (Δ_{Cu}). The stator parameters were kept identical for all evaluated cases, while the copper-layer thickness Δ_{Cu}, was varied within the range of 0–0.002 m, the range of which is based on calculations reported in.[35] In addition, the stator winding was designed with a three-phase star connection. The stator core was manufactured from grade 2013 electrical steel laminations. The stator was mounted on the moving vehicle, whereas the secondary element remained stationary.

Since the LIMs under consideration are analyzed from the point of view of their application in transportation systems, the results of studies of LIMs used in transportation systems for various purposes were taken into account when choosing the initial conditions of the LIM with a copper-coated solid secondary element.[5,8,40,41] In contrast to the previous study,[35] which primarily focused on the parameters of the secondary element and the thrust force of the LIM, the present work evaluates an extended set of LIM characteristics. In particular, operating slip, critical slip, thrust force, linear velocity of the vehicle, power factor, and efficiency are determined based on the equivalent circuit parameters under steady-state operating conditions. The copper-layer thickness is treated as a variable parameter influencing the electromagnetic characteristics of the system. The complete numerical dataset, including the input parameters and calculation results, is provided in Annex 2.[42] The initial parameters of the LIM are presented in Table 2.

4. Results and discussion

The parameters were calculated sequentially in accordance with the procedure described in the methods section and,[35–38] starting from equivalent circuit parameter identification and proceeding to force, slip, and performance evaluation. The calculated parameters of the investigated LIMs stator are summarized in Table 3.

Table 2. Initial conditions of the LIM.

LIM parameter	Symbol	Unit	Value
Initial conditions			
Thrust force	F_T	N	5000
Linear speed of traveling magnetic field	v_s	m/s	10
Air gap	δ	m	0.002
Vehicle mass	M	kg	5000
Stator length	l	m	1
Supply frequency	f_s	Hz	50
Supply phase voltage	U_{ph}	V	220
Number of stator modules	N_M	-	2
Number of winding phases	m	-	3

Note: Table 2. presents the initial parameters used for the LIM calculations described in Annex 2. These parameters define the initial operating conditions, electrical and design parameters of the LIM model used in the calculations.

Table 3. Calculated parameters of the LIM.

LIM parameter	Symbol	Unit	Value
Calculated parameters			
System power	P'	kW	72.6
Pole pitch	τ	m	0.1
Number of pole pairs	p	-	5
Effective core length	l_δ	m	0.1
The rated current of the traveling field winding section	I_{1nom}	A	54.99
Active resistance of the phase winding	r_1	Ohm	0.111
Reactive resistance of the phase winding	x_1	Ohm	0.409
Slot width	b_s	m	0.0167
Slot height	h_s	m	0.0448
Air gap magnetic flux density	B_δ	T	1.1
Total number of slots	z_{total}	-	30
Number of turns per phase	W_1	-	145
Active resistance of the iron secondary element	r'_{20}	Ohm	1.28
Reactive resistance of the secondary element	x'_{20}	Ohm	0.768

Note: Table 3. presents the calculated parameters of the LIM obtained using the initial parameters listed in Table 2. and the calculation methodology described in Annex 1.. The calculated parameters include the main electrical, magnetic, and geometric characteristics of the LIM. These parameters are subsequently used in the analysis of the LIM operating characteristics and are also provided in Annex 2.

Table 4. presents the calculated operating slips (s_{op}), thrust forces (F_{Top}), linear speeds of vehicle (v_{op}), power factors ($cos\varphi_{op}$), efficiencies (η_{op}), and critical slips (s_{cr}) of the LIM.

As shown in Table 4, compared with an LIM using a solid iron secondary element ($\Delta_{Cu} = 0$), increasing the copper-layer thickness of the copper-coated secondary element results in a decrease in critical and operating slips from 0.443% to 7.17% and from 0.77% to 6.18%, respectively. At the same time, operating velocity and efficiency increased from 0.83% to 6.64% and from 0.255% to 3.32%, respectively. The operating power factor also shows a slight increase, from 0.534 to 0.542, corresponding to an overall increase of approximately 1.49%. (Figure 2, Figure 3).

According to the operational thrust force results presented in Table 4, compared with the LIM using a solid iron secondary element (baseline value: $\Delta_{Cu} = 0$), the introduction of a copper layer initially results in a 0.08% decrease in thrust force, with the minimum value observed at $\Delta Cu = 0.0001$ m. With a further increase in copper layer thickness, the thrust force

Table 4. Parameters of the LIM with and without a copper-coated secondary element.

Δ_{Cu}, m	Parameters of LIM					
	s_{cr}	s_{op}	F_{Top}, N	v_{op}, m/s	$cos\varphi_{op}$	η_{op}
0 (St-3)	13.53	0.518	2335.6	4.82	0.534	0.391
0.0001	13.47	0.513	2333.7	4.86	0.534	0.392
0.0002	13.43	0.514	2344.2	4.85	0.535	0.392
0.0004	13.33	0.512	2352.3	4.88	0.536	0.393
0.0005	13.28	0.507	2349.7	4.93	0.536	0.394
0.0006	13.23	0.508	2360.4	4.92	0.537	0.394
0.0008	13.13	0.505	2368.3	4.95	0.538	0.396
0.001	13.03	0.502	2376.1	4.98	0.538	0.397
0.0015	12.79	0.491	2387.8	5.08	0.539	0.401
0.002	12.56	0.486	2411.9	5.14	0.542	0.404

Note: Table 4. presents the calculated operating parameters of the LIM for different copper layer thicknesses. The parameters include critical slip, operating slip, operating thrust force, vehicle operating velocity, operating power factor and operating efficiency. The case of $\Delta_{Cu} = 0$ corresponds to the uncoated St-3 secondary element, while the remaining cases correspond to different copper layer thicknesses. These parameters obtained from calculations presented in Annex 2.. The data presented in Table 4. are used to construct the graphs shown in Figure 2., Figure 3. and Figure 4..

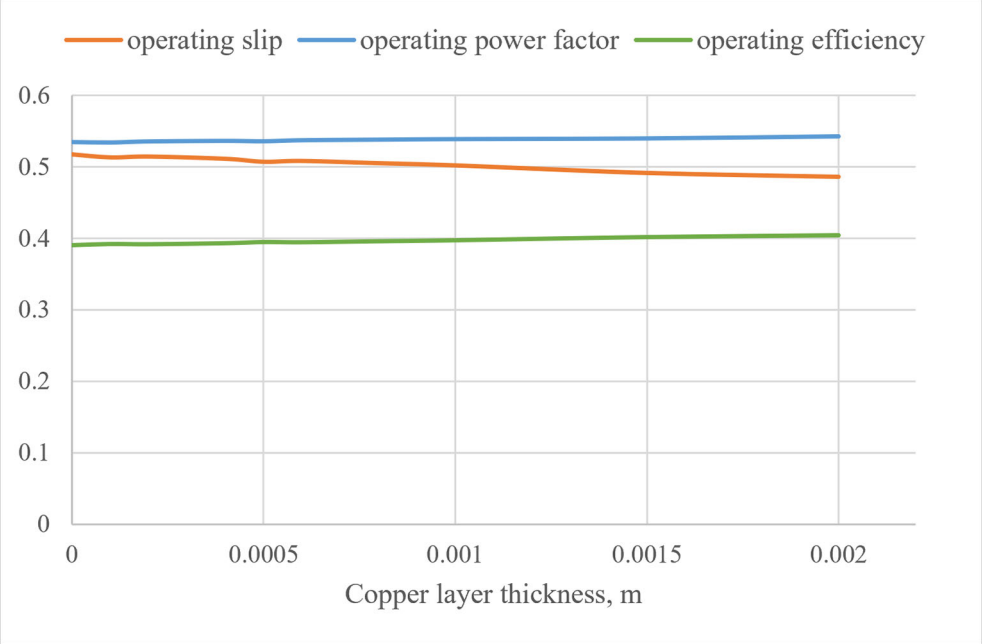

Figure 2. Dependence of operating slip (s_{op}), power factor ($cos\varphi_{op}$) and efficiency (η_{op}) on copper layer thickness Δ_{Cu}. The figure shows the dependence of the operating slip, power factor, and efficiency on the copper layer thickness. The case of $\Delta_{Cu} = 0$ corresponds to a solid secondary element without a copper coating. The copper layer thickness varies over the range from 0.0001 m to 0.002 m using the following values: 0.0001, 0.0002, 0.0004, 0.0005, 0.0006, 0.0008, 0.0010, 0.0015, and 0.002 m. The figure illustrates the variation of the operating parameters with increasing copper layer thickness. The values for graph are taken from Table 4.

generally increases, reaching its maximum value at 0.002 m, corresponding to an increase of approximately 3.27% relative to the baseline value (Figure 4). A minor local decrease in thrust force is observed between $\Delta_{Cu} = 0.0004$ m and 0.0005 m, where the thrust force decreases from 2352.3 N to 2349.7 N, corresponding to approximately 0.11%. This small variation does not alter the general tendency of increasing thrust force with copper layer thickness. The observed increase in thrust force may be associated with changes in the effective conductivity of the secondary element, current redistribution and changes in the interaction between the magnetic field and the secondary element. The initial decrease in

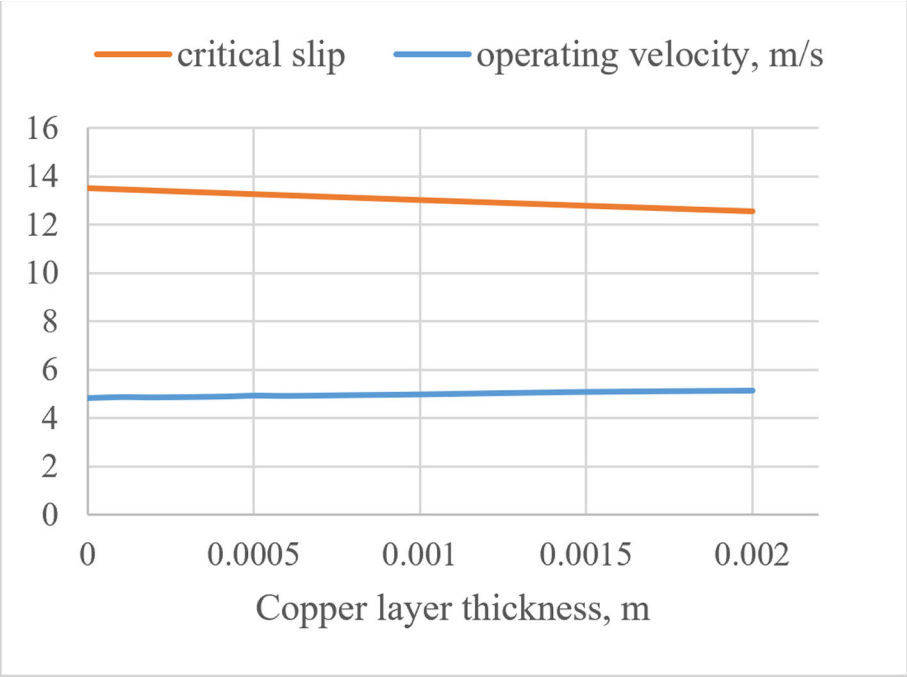

Figure 3. Dependence of operating velocity of vehicle (v_{op}) and critical slip (s_{cr}) on copper layer thickness Δ_{Cu}. The figure shows the dependence of the operating velocity of the vehicle and the critical slip on the copper layer thickness. The figure illustrates how the operating velocity and critical slip vary with increasing copper layer thickness. The values of graph were demonstrated in Table 4. and the copper layer thickness varies from 0.0001 m to 0.002 m using the same discrete thickness values as those considered in Figure 2.

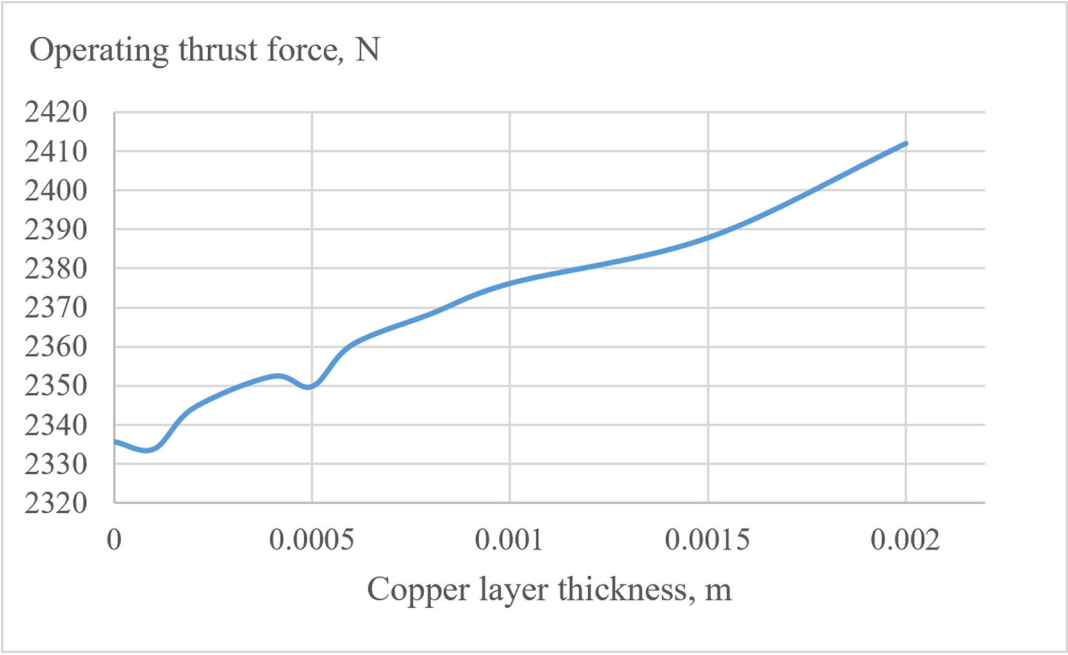

Figure 4. Dependence of operating thrust force (F_{Top}) on copper layer thickness Δ_{Cu}. The figure shows the dependence of the operating thrust force on the copper layer thickness. The figure illustrates how the operating thrust force varies with increasing copper layer thickness. The values of graph were demonstrated in Table 4. and the copper layer thickness varies from 0.0001 m to 0.002 m using the same discrete thickness values as those considered in Figure 2 and Figure 3.

thrust force followed by its subsequent increase with increasing copper-layer thickness requires further investigation. As shown in,[43] the skin depth of an electromagnetic wave in copper at 50 Hz is on the order of centimeters and decreases with increasing frequency. The field amplitude inside a conductor decays exponentially with depth. In practical applications, the effective penetration depth may be smaller than the theoretical value due to material properties and non-ideal conditions.[43] Although the skin depth exceeds the coating thickness, the mechanism underlying the observed thrust force trend requires further investigation and FEM validation.

The observed improvement in the LIM parameters is presumably primarily attributed to the reduction in the active resistance of the secondary element, which in turn reduces slip and improves traction, efficiency and speed of vehicle. Reduction of the active resistance of the secondary element was described in.[35] The copper layer increases the electrical conductivity of the secondary element, thereby improving electromagnetic coupling between the secondary element and the stator, which contributes to an increase in the power factor. Additionally, the observed improvement in efficiency may be attributed to reduced losses in the secondary element. However, given the calculation data, it is necessary to determine the optimal copper layer thickness, thermal and mechanical effects, as well as edge effects. The validation of results is planned for subsequent studies using experimental setups and FEM analysis.

Based on the obtained calculation results, it can be concluded that a copper-coated secondary element can be effectively applied in LIMs intended for transportation systems requiring high thrust force and speed to facilitate the acceleration of the train. Such operating conditions are typical during start-up of heavily loaded train units or when operating on track sections with steep track gradients, where increased traction force and speed is required. These conditions are particularly relevant in regions with complex terrain, such as Armenia, where mountainous landscapes and variable elevation profiles impose additional traction demands on rolling stock. In such cases, the use of copper coated secondary elements may be considered for specific track sections, although the practical implementation of such solutions requires further technical and economic evaluation. The observed increase in thrust force can also be advantageous in conveyor and elevator drive systems, particularly under conditions involving short-term overloads. In such applications, copper-coated secondary elements may be used to enhance performance during peak load periods, with conventional designs applied under normal operating conditions. Such operational scenarios are common in industrial sectors including mining, metallurgy, construction materials production and logistics, where variable loads and transient operating regimes frequently occur.

Linear induction motors can be considered to replace permanent-magnet-based drives in applications where high thrust at low speeds and robustness are more critical than maximum efficiency, such as heavy transport systems, conveyors, and harsh-environment operations. The obtained results demonstrate that the use of copper-coated secondary elements indicates potential performance improvements while maintaining a fully rare-earth-free design. Rare-earth elements are also associated with supply-chain risks and environmental concerns, which motivate the development of alternative motor technologies. From a resource-efficiency perspective, the use of copper may also be advantageous in regions with abundant reserves, such as Armenia, which possesses significant copper resources. The utilization of locally available raw materials can reduce dependence on external supply chains and support the development of energy-efficient electromechanical systems aligned with national sustainability and industrial resilience goals.

5. Conclusion

The analysis presented in this study demonstrates that the use of copper-coated solid secondary elements is a promising approach to improving the performance of LIMs. The application of such coatings enables an increase in thrust force and favorable changes in electromagnetic characteristics, without requiring significant structural modifications of the secondary element. This study highlights the potential of LIMs as a rare-earth-free alternative to permanent-magnet-based drive systems in transportation and industrial applications. The increasing of the copper layer thickness shows the positive impact on LIMs electromagnetic parameters. However, the optimization of the copper layer thickness remains a critical factor, requiring further investigation. Additional studies should focus on the thermal and mechanical effects associated with the coating, as well as on the long-term reliability and practical implementation of this approach. The validation of results is planned for subsequent studies using experimental setups and FEM analysis.

Ethics and consent

Ethical approval and consent were not required.

Data availability

The data and calculation materials supporting the findings of this study are openly available in:

1. Zenodo: Calculation methodology of the double-sided linear induction motor. https://zenodo.org/records/22980391; DOI https://doi.org/10.5281/zenodo.22980391.[38] This dataset contains the methodology,

equations, and calculation procedures used to obtain the reported results. It contains the following underlying data: Annex 1. Calculation methodology of the double-sided linear induction motor.docx

Data are available under the terms of the Creative Commons Attribution 4.0 International license (CC-BY 4.0).

2. Zenodo: Parameter calculations for the double-sided linear induction motor. https://zenodo.org/records/22980349; DOI https://doi.org/10.5281/zenodo.22980349.[42] This dataset contains the complete numerical data and calculation results underlying the analyses reported in this article. It contains the following underlying data: Annex 2. Parameter calculations for the double-sided linear induction motor.xlsx

Data are available under the terms of the Creative Commons Attribution 4.0 International license (CC-BY 4.0).

Acknowledgements

We would like to thank Mattia De Rosa (PhD Mechanical Engineering. Associate professor in Energy and Thermal Engineering at the University of Genoa, EU Horizon Europe STREACS project supervisor.) for his support within the structural advisory and writing this paper.

References

1. Solomin VA, Zamshina LL, Solomin AV: *Linear asynchronous traction motors for high-speed rolling stock and their mathematical modeling.* Moscow: FGBOU UMC ZHDT; 2015; 164. (In Russian).
Reference Source

2. Gieras JF: *Linear induction drives.* Oxford, UK: Oxford University Press; 1994; 292.
Reference Source

3. Vintizenko I: *Linear induction accelerators for high power microwave devices.* Boca Raton, FL, USA: CRC Press;1st ed 2018; 436.
Publisher Full Text

4. European Commission: **Critical raw materials.** *European Commission.* 2026.
Reference Source

5. Veselovskiy ON, Konyayev AY, Sarapulov FN: *Linear asynchronous motors.* Moscow, Energoatomizdat; 1991; 256. (In Russian).
Reference Source

6. Ryabtsev I, Fomichov S, Kuznetsov V, *et al.*: *Surfacing and additive technologies in welded fabrication.* Springer; 2023; 226.
Publisher Full Text

7. Postnikov IM: **Designing of electrical machines. Gos. publishing house in technical letter.** *USSR Kyiv.* 1960; 909. (In Russian).
Reference Source

8. Boldea I: *Linear electric machines, drives, and Maglevs handbook.* CRC Press;Second ed 2023; 718.
Reference Source

9. Kaye RJ, Masada E: **Comparison of linear synchronous and induction motors.** *Urban Maglev technology development program Colorado Maglev project Project Report.* 2004; 22.
Reference Source

10. Antonov YF, Zaitsev AA: *Magnetic levitation transport technology.* Gapanovich VA, editors. Moscow, FIZMATLIT: 2014; 476. 978–5–9221-1540-7. (In Russian).
Reference Source

11. Stumberger G, Zarko D, Aydemir MT, *et al.*: **Design and comparison of linear synchronous motor and linear induction motor for electromagnetic aircraft launch system.** *Proceedings of the IEEE International Electric Machines and Drives Conference.* USA, Madison, WI: 1–4 June 2003; **1**: 494–500.
Reference Source

12. Zhou B, Li Z, Zhao Y, *et al.*: **Rare earth elements supply vs. clean energy technologies: new problems to be solve.** *Gospodarka Surowcami Mineralnymi - Mineral Resour. Manag.* 2016; **32**: 29–44.
Publisher Full Text

13. Binnemans K, Jones PT, Blanpain B, *et al.*: **Recycling of rare earths: a critical review.** *J. Clean. Prod.* 2013; **51**: 1–22.
Publisher Full Text

14. Ya.M. K: **Method of manufacturing a magnetic circuit.** *All-Union Scientific Research, Planning-Design and Technological Institute of Electrical Machine Building.*Author's Certificate: SU 1480021 A1, published 15.05.1989. Application №4145185 filed 10.11.1986. (In Russian).
Reference Source

15. Shumov YN: **High-speed and ultra-high-speed asynchronous machines abroad: a review of publications.** *Elektrichestvo.* 2011; **5**: 36–41. (In Russian).
Reference Source

16. Wang S, Miao D-M, Shen J-X: **Optimal design of a linear induction motor for woodworking machine application.** *17th International Conference on Electrical Machines and Systems (ICEMS).*Hangzhou, China: 2014; 3633–3637.
Reference Source

17. De Oliveira RAH, Berger D, Schultz L, *et al.*: **Finite element analysis of the forces developed on linear induction motors.** *In Proceedings of the 2015 IEEE 13th Brazilian Power Electronics Conference and 1st Southern Power Electronics Conference (COBEP/SPEC).* Fortaleza, Brazil; 29 November-2 December 2015; 1–6.
Reference Source

18. Sarapulov FN, Smolianov IA, Rodionov IE: **Investigation of the traction linear induction motor for conveyor train.** *Russian Internet Journal of Electrical Engineering.* 2018; **5**(1): 34–37. (In Russian).
Publisher Full Text

19. Sarapulov FN, Smolyanov IA, Tarasov FE: **Study of the linear induction motor with bimetallic secondary element.** *Acta Technica CSAV.* 2018; **63**(2): 205–220.
Reference Source

20. Mahto MK, Kumar A, Raja AR, *et al.*: **Cladding of copper sheet on mild steel using friction stir welding.** *Int. J. Adv. Manuf. Technol.* 2021; **118**(9–10): 3345–3360.
Publisher Full Text

21. Schlesinger M, Paunovic M: *Modern electroplating.* John Wiley & Sons; 5th ed 2010; 752.
Reference Source

22. Privalov AS: **Features of cold gas-dynamic spraying as a technology for preserving the original properties of deposited materials.** *In collection of scientific articles of the VIII International Youth Scientific Conference "Youth and Knowledge - a Guarantee of Success".* Gorokhov AA, Kursk, editors. 2021; **3**: 323–328. (In Russian).
Reference Source

23. Arkhipov VE, Londarskiy AF, Moskvitin GV: *Gas dynamic spraying: Structure and properties of coatings.* Moscow: Krasand Publ; 2017; 239. (In Russian).
Reference Source

24. Arkhipov VE, Londarskiy AF, Moskvitin GV, *et al.*: **Application of copper coatings on steel by gas-dynamic spraying.** *Metalloobrabotka.* 2012; **2**(68): 13–17. (In Russian).
Reference Source

25. Kozlov IA, Leshchev KA, Nikiforov AA, *et al.*: **Cold spray coatings (review).** *Trudy VIAM.* 2020; **8**(90): 77–93. (In Russian).
Publisher Full Text

26. Assadi H, Gärtner F, Stoltenhoff T, *et al.*: **Bonding mechanism in cold gas spraying.** *Acta Mater.* 2003; **51**(15): 4379–4394.
Publisher Full Text

27. Schmidt T, Gaertner F, Kreye H: **New Developments in cold spray based on higher gas and particle temperatures.** *J. Therm. Spray Technol.* 2006; **15**(4): 488–494.
Publisher Full Text

28. Champagne VK: *The cold spray materials deposition process.* Woodhead Publishing; 2007; 362p.
Publisher Full Text

29. Grujicic M, Zhao CL, DeRosset WS, *et al.*: **Adiabatic shear instability based mechanism for particles/substrate bonding in cold-spray process.** *Mater. Des.* 2004, December 2004; **25**(8): 681–688.
Publisher Full Text

30. Stoltenhoff T, Borchers C, Gaertner F, *et al.*: **Microstructures and key properties of cold-sprayed and thermally sprayed copper coatings.** *Surf. Coat. Technol.* 2006; **200**: 4947–4960.
Publisher Full Text

31. Yin S, Suo X, Guo Z, *et al.*: **Deposition features of cold sprayed copper particles on preheated substrate.** *Surf. Coat. Technol.* 2015; **268**: 252–256.
Publisher Full Text

32. Villafuerte J: *Modern cold spray: materials, process, and applications.* Cham, Switzerland: Springer International Publishing; 2015; 429.
Publisher Full Text

33. Xiao M, Qiang X, Jiang F: **Effect of copper addition on the phase composition and microstructure evolution of Fe-based amorphous alloy coatings prepared by laser cladding.** *Adv. Mater. Sci. Eng.* 2022; **2022**: 1–7. Article ID 3511432.
Publisher Full Text

34. Gnedenkov AS, Nomerovskii AD, Tsvetnikov AK, *et al.*: **Formation of the composite polymercontaining coatings on St3 steel using cold gas dynamic spraying technology.** *Vestnik of the FEB RAS.* 2022; 6: 35–45. (In Russian).
Reference Source

35. Mayilyan AL, Saghatelyan MA, Khangeldyan AG: **Calculating the parameters of a linear asynchronous machine with a secondary element covered with a copper layer.** *Proceedings National Polytechnic University of Armenia: Electrical engineering, Energetics, Yerevan.* 2023; **1**: 68–79. (In Russian).
Reference Source

36. Kutsevalov VM: *Asynchronous and synchronous machines with massive rotors.* Moscow, Energiya: 1979; 160. (In Russian).
Reference Source

37. Mayilyan AL, Saghatelyan MA, Khangeldyan AG: **Improving the parameters of a linear induction motor with a massive secondary element.** *Proceedings National Polytechnic University of Armenia: Electrical engineering, Energetics, Yerevan.* 2024; **1**: 19–30. (In Russian).
Reference Source

38. Khangeldyan A: Calculation methodology of the double-sided linear induction motor. [Dataset]. *Zenodo.* 2026.
Publisher Full Text

39. Kopylov IP, Klokov BK, Morozkin VP, *et al.*: *Designing of electrical machines: textbook.* Moscow, Yurait:4th ed. 2011; 767. (In Russian).
Reference Source

40. Epifanov AP, Kril DB: **Linear asynchronous electric drive of the monorail transport system for feeding in livestock farms.** *Izvestiya of the Saint-Petersburg State Agrarian University.* 2022; **66**(1): 113–124. (In Russian).
Reference Source

41. Zhang Q, Liu H, Song T, *et al.*: **A novel, improved equivalent circuit model for double-sided linear induction motor.** *Electronics.* 2021; **10**: 1644.
Publisher Full Text

42. Khangeldyan A: Parameter calculations for the double-sided linear induction motor. [Dataset]. *Zenodo.* 2026.
Publisher Full Text

43. Demirchyan KS, Neiman LR, Korovkin NV, *et al.*: **Theoretical foundations of electrical engineering.** *Textbook for universities.* Saint Petersburg:4th ed. 2003; **3**: 377. Electromagnetic field theory.
Reference Source (In Russian)